Hot deformation of spray formed nickel-base superalloy using processing maps

KANG Fu-wei(康福伟)[1, 2], ZHANG Guo-qing(张国庆)[3], LI Zhou(李 周)[3], SUN Jian-fei(孙剑飞)[1]

1. School of Materials Science and Engineering, Harbin Institute of Technology, Harbin 150001, China;
2. School of Materials Science and Engineering, Harbin University of Science and Technology, Harbin 150040, China;
3. Beijing Institute of Aeronautical Materials, Beijing 100095, China

Abstract: The hot compression testing of hot isostatically pressed(HIPed) spray formed(SF) nickel-base superalloy was carried out by thermal mechanical simulator in the temperature range of 1 050−1 140 ℃ at strain rates of 0.01−10 s^{-1} and engineering strain of 50%. A processing map was developed on the basis of these data by using the principles of dynamic materials modeling. The microstructural evolution of deformed samples was also examined on the basis of optical and electron microscopic observations. The map exhibits two domains: the instability domain at the temperatures of 1 050 ℃−1 110 ℃ and strain rate of 0.01 s^{-1}, the stability domain at the temperatures of 1 110 ℃−1 140 ℃ and strain rates of 1 s^{-1}−10 s^{-1}, with a peak efficiency of about 40%. The dynamic recrystallization(DRX) is observed in the stability domain and the deformed specimens are no cracking or instabilities. However, there is no DRX in the instability domain and the alloy exhibits flow instability with cracks due to poor workability. The optimum hot working condition was determined in the stability domain.

Key words: spray forming; nickel-base superalloy; hot compression; processing map; recrystallization

1 Introduction

The nickel-base superalloys have been extensively used for aerospace applications because of the attractive combination of properties such as high strength, corrosion resistance, and fatigue strength[1]. Their high temperature strength is achieved primarily by solid solution strengthening of γ' phase (Ni$_3$Al(Ti,Nb)). Unfortunately, it is rather difficult to deform for some as-cast nickel-base superalloys with high alloying elements content and complex system of phases in the microstructure, so they only can be hot worked into very narrow processing windows, in terms of temperature and strain rate. Powder metallurgy(P/M) processing generally yields fine and homogeneous microstructures, but its disadvantage is the susceptibility for impurity contamination. The alloy investigated in this work was produced by spray forming(SF) route, which had the advantages of reducing segregation of alloying elements, distributing the carbides and other microconstituents more uniformly in the matrix, and producing finer grain size[2]. Although several studies have focused on the hot

deformation behaviour of spray formed alloys[3−8], little has been published on the characterization of hot deformation in a spray formed nickel-base superalloy using processing maps.

In this study, the approach of processing map is adopted to analyse the deformation behaviour of as-HIPed SF nickel-base superalloy during hot deformation. The changes of microstructure associated with different test conditions during the deformation processing are also investigated.

2 Experimental

The alloy investigated was a precipitation-hardened superalloy by the formation of intermetallic compound γ' Ni$_3$(Al,Ti), with a high volume fraction of about 35% and a solvus temperature of 1 130 ℃. By the spray forming process, the spray formed billet was prepared, with a diameter of 100 mm and height of 95 mm. The chemical composition was as follows (mass fraction, %): 11.06 Cr, 4.55 Mo, 14.4 Co, 2.64 W, 2.59 Ti, 2.74 Nb, 3.12 Al and balance Ni. To improve the density of the spray formed billet, it was HIPed at 1 120 ℃ for 2 h in

argon atmosphere at a pressure of 130 MPa. The cylindrical compression specimens of 8 mm in diameter and 12 mm in height were machined from the as-HIPed billet. Hot compression testing was conducted in the temperature ranging from 1 050 ℃ to 1 140 ℃ at 30 ℃ intervals and constant strain rate ranging from 0.01 s^{-1} to 10 s^{-1} at intervals of an order of magnitude. All specimens were deformed to 6 mm in height and nitrogen-cooled immediately for microstructural observation. To measure accurately the temperature of the specimen during deformation, a thermocouple was welded on the specimen surface at half its height. To minimize the friction between the specimen and dies, the MoS$_2$ solution was used as lubricant.

To observe the evolution of microstructure during compression tests, the deformed specimens were sectioned parallelly to the compression axis and prepared for metallographic examination using standard procedures. The metallographic samples were etched using a solution of H$_2$SO$_4$(5 mL)+CuSO$_4$(20 g)+HCl (100 mL)+H$_2$O(10 mL). The microstructures of the deformed samples were observed on GX71–6230A type optical microscope and Quanta 200 type scanning electron microscope.

3 Results and discussion

3.1 Initial microstructure

The microstructures of the spray formed and as-HIPed SF nickel-base superalloy are shown in Fig.1. The superalloy consists of fine-equiaxed γ grains with an average diameter of 30 μm. A few porosities are presented at the grain boundary triple junctions, as shown in Fig.1(a). The microstructure of as-HIPed SF alloy is shown in Fig.1(b), in which most of porosities are closed and the grain size is slightly increased. The SEM examination of the specimen reveals that the fine γ′ phases (Ni$_3$Al(Ti,Nb)) are uniformly distributed in matrix γ (Fig.1(c)).
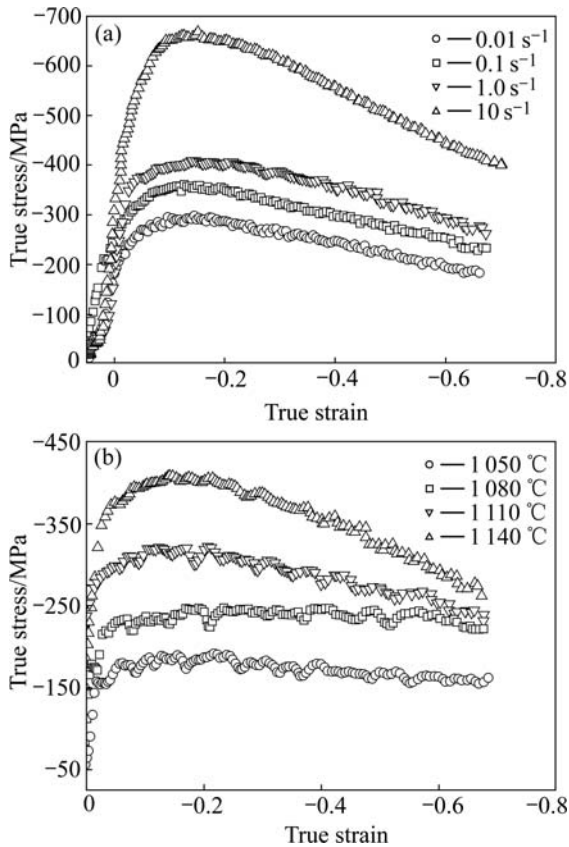
3.2 Stress—strain curves

The typical true stress—true strain curves of the as-HIPed SF nickel-base superalloy are presented in Fig.2. The shapes of the true stress—strain curves are in agreement with the usually observed deformation characteristics of nickel-base superalloys[9−10]. The flow stress at a given strain increases with decreasing the temperature and increasing the strain rate, thereby exhibiting typical characteristics metals deformed in hot compression conditions. The flow stress increases to a peak with increasing strain and then decreases as the strain further increases, which is more significant at lower temperature and higher strain rates. The initial rapid rise in stress is associated with an increase in
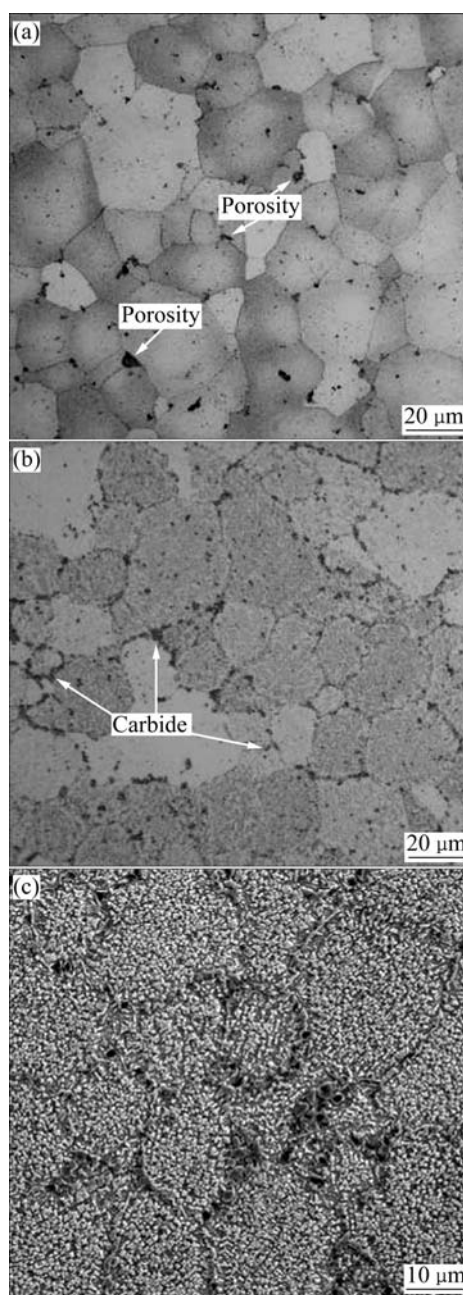
Fig.1 Microstructures of spray formed and as-HIPed SF nickel-base superalloy: (a) Optical micrograph of spray formed superalloy; (b) Optical micrograph of as-HIPed spray formed nickel-base superalloy; (c) SEM image of as-HIPed spray formed nickel-base superalloy

dislocation density resulting from work hardening. Particularly at high strain rate, the flow softening behavior or stress drop in the stress—strain curves indicates the generation of dynamic recrystallization, dynamic recovery, or cracks during hot compression. In the alloys with low or intermediate stacking fault energy, e.g. nickel or stainless steel, the dynamic recovery proceeds slowly[11]. Therefore, the dynamic recrystallization and the formation of cracks may be important causes of the decrease in flow stress.

Fig.2 True stress—strain curves of as-HIPed spray formed nickel-base superalloy: (a) At 1 050 ℃ with different strain rates; (b) With 1.0 s^{-1} at different testing temperatures

3.3 Processing map

The dynamic material model(DMM) is used to construct processing maps for the as-HIPed SF nickel-base superalloy. The basis and principles of the processing maps approach have been described earlier [12], and it has been successfully applied to optimize hot workability in a number of commercial alloys like Nimonic AP-1, IN718, AISI304L stainless steel and Zircaloy[13]. In brief, the rate of microstructural change is given by the dimensionless parameter called the efficiency of power dissipation[14]:

$$\eta = \frac{2m}{m+1} \qquad (1)$$

where m is the strain rate sensitivity of flow stress, and η is the efficiency of power dissipation. This parameter may be plotted as a function of temperature and strain rate to obtain the power dissipation map. The power dissipation map shows isoefficiency contours, which represent the relative rate of entropy production occurring in the material due to microstructural dissipation[14].

The continuum instability criterion for identifying the domains of flow instabilities, has been developed on

the basis of the extremum principles of irreversible thermodynamics as applied to large plastic flow and given by another dimensionless parameter[14]:

$$\xi(\dot{\varepsilon}) = \frac{\partial \ln \dfrac{m}{m+1}}{\partial \ln \dot{\varepsilon}} + m < 0 \qquad (2)$$

The $\xi(\dot{\varepsilon})$ parameter may the evaluated as a function of temperature and strain rate to obtain an instability map, where metallurgical instability during plastic flow occurs in domains $\xi(\dot{\varepsilon}) < 0$. The power dissipation map is superimposed on the instability map to constitute a processing map, which exhibits domains with local efficiency maxima representing certain specific microstructural mechanisms together with domains of flow instabilities. Therefore, the processing map must be related to the microstructure evolution[15].

On the basis of flow stress data given in Fig.2, the processing map of the as-HIPed SF nickel-base superalloy generated at the strain of 0.5 is shown in Fig.3. The map is clearly classified into two domains, e.g. the instability deformation domain and the stability deformation domain, as shown in Fig.3. The instability domain occurs in the temperature range of 1 050 ℃ to 1 110 ℃ and strain rate of 0.01 s^{-1}, and the stability domain in the temperature range of 1 110 ℃ to 1 140 ℃ and strain rate above 1.0 s^{-1}. In the stability domain, with the increasing of deforming temperature and strain rate, the η value gradually increases, up to its peak efficiency of about 40%, indicating that the domain may be an optimum condition for hot deformation of this alloy. The microstructural evolution mechanisms corresponding to the two domains are identified and correlated with the flow behavior in the following section.
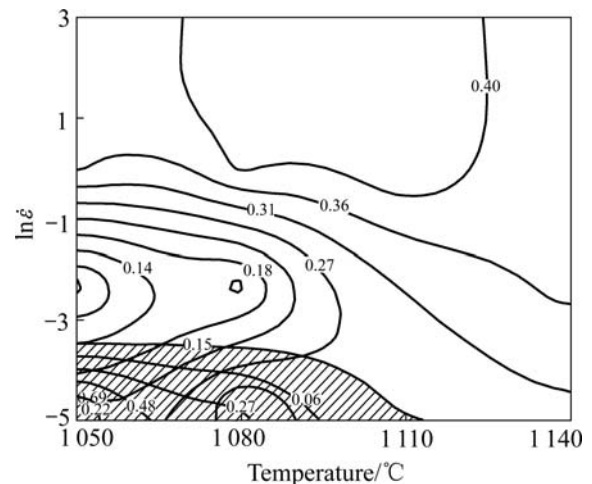
Fig.3 Processing map of as-HIPed spray formed nickel-base superalloy at strain of 50% (Shaded area represents instability domain, and the other area represents stability domain. The contours represent isoefficiency of power dissipation expressed in percent[16])

3.3.1 Instability domain

The instability domain predicts that the material will undergo flow instability at temperature below 1 110 ℃ and strain rates below 0.1 s^{-1}. Specimens deformed at the domain exhibit cracks along the circumference running in the direction of the compression axis, and the microstructure consists of dead metal zones and deformed zone, as shown in Fig.4(a). From Figs.4(b) and (c), it is clearly indicated that there are only elongated grains in the deformed zone and undeformed grains in the dead metal zones, instead of the dynamic recrystallized structure.
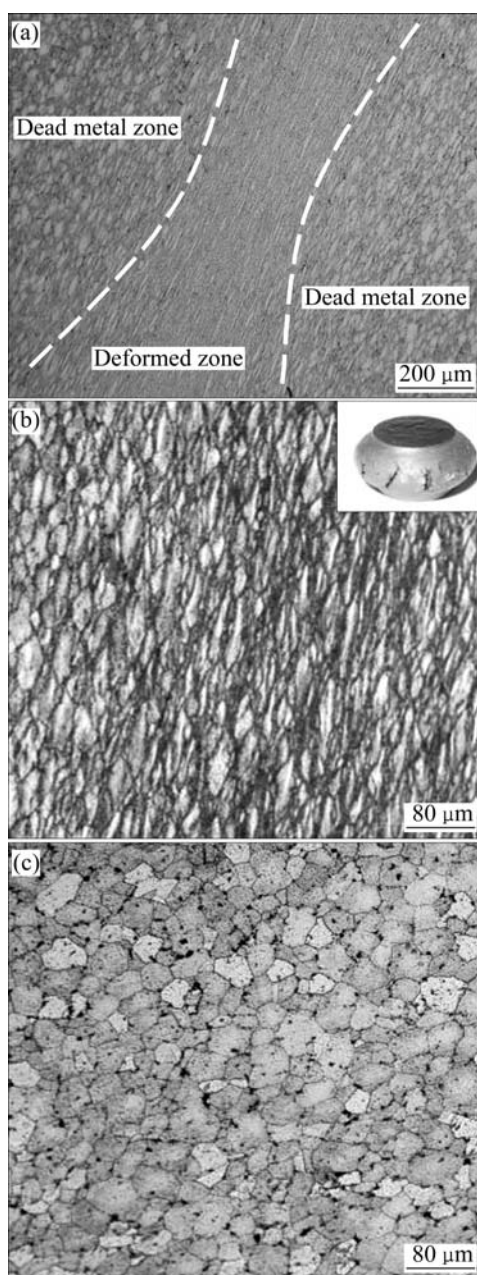
Fig.4 Microstructures of deformed specimens in instability domain 0.01 s^{-1}, 1 050 ℃: (a) Dead metal zones and deformed zone; (b) Fibre grains in deformed zone; (c) Undeformed grains in dead metal zones

The most probable deformation mechanism is the sliding of grain boundaries, which significantly contributes to the total strain for the fined grain alloy[10]. The consequence of the grain boundary sliding process depends upon the accommodation mechanism at the grain boundary triple junctions, where considerable stress concentration is caused by the sliding of the neighboring grains. If the rate of stress concentration is beyond the rate matching the rate of grain boundary sliding, surface cracking will occur, as shown in Fig.4(b) (right top corner). Thus, it may be concluded that the lower strain rate domain represents a cracking mechanism. Compared with hot deformation of many alloys, the characteristic of hot deformation for the as-HIPed SF nickel-base superalloy presents an abnormal relationship with strain rate, namely the hot workability increases as strain rate rises. This is partly because grain boundaries sliding is relatively diminished and partly because dynamic recrystallization proceeds more rapidly even though it initiates at a higher strain. The consequence is in consistent with the hot deformation feature of 301 stainless steels and P/M superalloy[17−18]. In view of the poor workability associated with this domain, it has to be strictly avoided in designing metal working processes for this superalloy.

3.3.2 Stability domain

The stability domain occurred at high strain rate (≥1.0 s^{-1}) and in the temperature range of 1 110 ℃ to 1 140 ℃ has a peak efficiency of about 40%, which is typical of the dynamic recrystallization process in nickel-base superalloy[14]. The microstructures of specimen deformed at the stability domain are shown in Fig.5, which exhibit dynamic recrystallization features. These include wavy or serrate grain boundaries and grain interiors, which are nearly free from annealing twins, as shown with arrows in Fig.5(a). The results of earlier investigations of processing maps on IN625 are in agreement with this interpretation[10]. Furthermore, the appearance of the deformed specimen observed under conditions in this domain also supports this interpretation. They exhibit smooth surface without cracks, as shown in Fig.5(b) (right top corner). This indicates that the workability is improved in this domain and the optimum conditions are obtained for hot deformation of the alloy used in this study.

4 Conclusions

1) The microstructure of as-HIPed SF nickel-base superalloy is characterized by fine equiaxed grain.

2) The instability domain occurs in the temperature range of 1 050 ℃ to 1 110 ℃ and strain rate of 0.01 s^{-1}, and the stability domain in the temperature range of 1 110 ℃ to 1 140 ℃ and strain rate range of 1.0 s^{-1} to
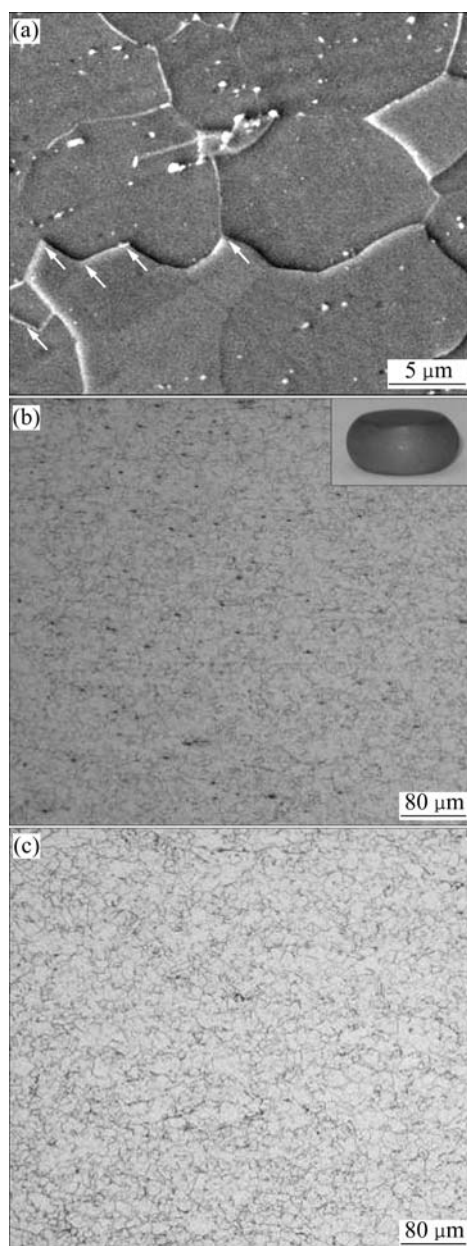
Fig.5 Microstructures of deformed specimens in stability domain: (a) 1.0 s^{-1}, 1 140 ℃, exhibiting wavy or irregular grain boundaries typical of DRX; (b) 10 s^{-1}, 1 110 ℃, fine recrystallization grains; (c) 10 s^{-1}, 1 140 ℃, fine recrystallization grains

10.0 s^{-1} according to its processing map.

3) The DRX is observed in the stability domain without cracking in the deformed specimens, while in the instability domain, the specimen cracks because DRX is absent.

4) The optimum hot deformation conditions for the alloy are the temperature ranging from 1 110 ℃ to 1 140 ℃, the strain rate ranging from 1.0 s^{-1} to 10 s^{-1} and engineering strain 50%.

References

[1]   FECHT H, FURRER D. Processing of nickel-base superalloys for turbine engine disc application[J]. Advanced Engineering Materials, 2002, 2(12): 777−787.

[2]   GRANT P S. Spray forming [J]. Progress in Materials Science, 1995, 39(4/5): 497−545.

[3]   RODENBURG C, KRZYZANOWSKI M, BEYNON J H, RAINFORTH W M. Hot workability of spray-formed AISI M3:2 high-speed steel [J]. Materials Science and Engineering A, 2004, 386(1/2): 420−427.

[4]   HANLON D N, LI Y H, RAINFORTH W M, SELLARS C M. Formability of spray-formed, high-chromium content, white cast iron [J]. Journal of Materials Science Letters, 1998, 17(19): 1637−1640.

[5]   CHEN C Y, TSAO CHI Y A. Spray forming of silicon added AZ91 magnesium alloy and its workability [J]. Materials Science and Engineering A, 2004, 383(1): 21−29.

[6]   FRANK S Y H, CHEN Y C, TASO C Y A. Workability of spray-formed 7075Al alloy reinforced with SiC$_p$ at elevated temperature [J]. Materials Science and Engineering A, 2004, 364(1/2): 296−304.

[7]   KIM W J, YEON J H, LEE J C. Superplastic deformation behavior of spray-deposited hyper-eutectic Al-25Si alloy [J]. Journal of Alloys and Compounds, 2000, 308: 237−243.

[8]   LI Zhou, ZHANG Guo-qing, ZHANG Zhi-hui, TIAN Shi-fan. Investigation into hot deformation behavior of spray formed superalloy GH742 [J]. Acta Metallurgica Sinica (English Letters), 2004, 17(2): 205−209.

[9]   MASHREGHI A R, MONAJATIZADEH H, JAHAZI M, YUE S. High temperature deformation of nickel base superalloy Udimet 520 [J]. Materials Science and Technology, 2004, 20(2): 161−166.

[10] MEDEIROS S C, FRAZIER W G, PRASAD Y V R K. Hot deformation mechanisms in a powder metallurgy nickel-base superalloy IN 625 [J]. Metallurgical and Materials Transactions A, 2000, 31(9): 2317−2323.

[11] ZHOU L X, BAKER T N. Effects of strain rate and temperature on deformation behaviour of IN 718 during high temperature deformation [J]. Materials Science & Engineering A, 1994, 177(1/2): 1−9.

[12] PRASAD Y V R K, GEGEL H L, DORAIVELU S M, MALAS J C, MORGAN J T, LARK K A, BARKER B R. Modeling of dynamic material behavior in hot deformation: forging of Ti–6242 [J]. Metallurgical Transactions A, 1984, 15(10): 1883−1892.

[13] SOMANI M C, MURALEEDHARAN K, PRASAD Y V R K, SINGH V. Mechanical processing and microstructural control in hot working of hot isostatically pressed P/M IN-100 superalloy [J]. Materials Science and Engineering A, 1998, 245: 88−99.

[14] PRASAD Y V R K, SASIDHARA S. Hot working guide a compendium of processing maps [M]. Materials Park, Ohio: ASM International, 1997: 5−9.

[15] HUANG Guang-sheng, WANG Ling-yun, CHEN Hua, HUANG Guang-jie, ZHANG Suo-quan. Hot deformation and processing maps of 2618 aluminum alloy [J]. The Chinese Journal of Nonferrous Metals, 2005, 15(5): 763−767. (in Chinese)

[16] KANG Fu-wei, SUN Jian-fei, ZHANG Guo-qing, LI Zhou. Characteristics of hot compression deformation and microstructure evolution of spray formed nickel base superalloy[J]. Acta Metallurgica Sinica, 2007, 43(10): 1053−1058.

[17] MCQEEN H J, YUE S, RYAN N D. Hot working characteristics of steels in austenitic state [J]. Journal of Materials Processing Technology, 1995, 53: 293−301.

[18] BHOWAL P R, BHATHENA N M. Development of a necklace microstructure during isothermal deformation and its properties relative to uniform microstructures [J]. Metallurgical Transactions A, 1991, 22: 1999−2008.

(Edited by YUAN Sai-qian)